MUTANT HUNTINGTIN BINDS THE MITOCHONDRIAL FISSION GTPASE DRP1 AND INCREASES ITS ENZYMATIC ACTIVITY

Wenjun Song[1], Jin Chen[1], Alejandra Petrilli[1], Geraldine Liot[1], Eva Klinglmayr[2], Yue Zhou[1],Patrick Poquiz[3], Jonathan Tjong[3], Mahmoud A. Pouladi[4], Michael R. Hayden[4], Eliezer Masliah[5], Mark Ellisman[3], Isabelle Rouiller[6], Robert Schwarzenbacher[2], Blaise Bossy[1], Guy Perkins[3], Ella Bossy-Wetzel[1*]

[1] Burnett School of Biomedical Sciences, College of Medicine, University of Central Florida, Orlando, FL; [2] Structural Biology Group, Department of Molecular Biology, University of Salzburg, Austria; [3]NCMIR, University of California, San Diego, CA; [4]Centre for Molecular Medicine and Therapeutics, University of British Columbia, Vancouver, BC, Canada; [5]University of California, San Diego, La Jolla, CA; [6]Department of Anatomy and Cell Biology, McGill University, Montreal, QC, Canada

Supplementary Information

Full Methods

Plasmids. The pDsRed2-Mito was obtained from Clontech. The DRP1 expression vector EX-M0235-M29 (NCBI accession number: NM_012062.3, with 736 amino acid residues, plus N-terminal EGFP tag) was purchased from GeneCopoeia. The huntingtin plasmids, pGW1-HTT exon1-Q17-GFP, pGW1-HTT exon1-Q46-GFP, and pGW1-HTT exon1-Q97-GFP, were from S. Finkbeiner and pcDNA3.1-Q25-GFP and pcDNA3.1- Q97-GFP from L. Thompson. The YFP-DRP1 construct was from R. Youle. The GST-HTT exon1-Q20 and GST-HTT exon1-Q53 constructs in pGEX-6p-1 were from U. Hartl. The pcDNA3- $DRP1^{K38A}$ plasmid and DRP1 (NCBI accession number: NM_005690.3) baculovirus were from Van der Bliek. The $MFN2^{RasG12V}$ (pro82-FzoRV12pECFP-C1) plasmid in which the P-loop residues are replaced with residues from the activated RasG12V was obtained from R. Slack. The pcDNA 3.1β-shRNA-Drp1 and pcDNA 3.1β-scramble were obtained from S. Strack.

Human lymphoblast, fibroblast, and brain tissue. Lymphoblast lines from HD individuals GM13508 (allele 1, 58Q), GM13509 (allele 1, 70Q), GM14044 (allele 1, 250Q) and from normal subjects GM00530 and GM09820, and untransformed fibroblasts from HD individuals GM05539 (onset at age 2 years), GM04693 (onset at age 41 years) and from normal subject I91L17, were obtained from the Coriell Institute for Medical Research and cultured following their recommendations. Human postmortem striatal

tissue was obtained from the Alzheimer's Disease Research Center at UCSD. Samples included in **Fig. 3**: HD diagnosis case # X5370, a 62-year-old person, female, 12 postmortem hours, case # X5374, a 69-year-old person, female, 12 postmortem hours, case # X5298, a 75-year-old person, female, case #X5348, a 62-year-old person, male, and case # X5302, an unaffected 83-year-old person, female, 72 postmortem hours.

Primary cortical neurons and transfection. Purified cortical cultures were prepared from E18 rat embryos[1,2]. Neuronal cultures (400,000 cells ml^{-1}) were transfected at 5 DIV with Lipofectamine 2000 (Invitrogen). Experiments were carried out two days after transfection.

Fixed and live cell imaging. Images were acquired with an Axiovert Zeiss 100M inverted fluorescence microscope equipped with a Plan Apochromat 63×1.4 NA oil objective, a DG-4/Lambda 10-2 combo Xe-arc illumination unit (Sutter), and a Sensicam QE cooled CCD camera (PCO AG) controlled by MetaMorph 7.1 software (Molecular Devices) as described[3]. To visualize DsRed2-Mito, the excitation filter was S555/28× (Chroma) and the emission filter was S617/73m (Chroma). To visualize EGFP, the excitation filter was S490/20× (Chroma) and the emission filter was S528/38m (Chroma). Three-dimensional images were acquired using the Multi Dimensional Acquisition module in MetaMorph 7.1 (2×2 binning, 0.2 μm step size, 15–20 z-planes). The z-series were de-hazed by MetaMorph 7.5 "remove haze" filtering followed by high-pass function in FFT (Fast Fourier Transform). Three-dimensional surface rendering was performed using Metamorph 4D-viewer with the proper threshold and images were saved and

exported as TIFF files. Images of fibroblasts were acquired using a laser confocal microscope (Leica TCS SP5) with a 40× oil HCXPLAPO objective using LAS AF software. Z-stacks of 1024×1024 d.p.i. images were obtained using a 543 HeNe laser with a step size of 0.3 μm. Representative image stacks were surface rendered using Metamorph 4D-viewer with proper thresholding. For live cell imaging, cortical neurons were grown on Lab-Tek II (#1.5 glass) 8-chamber slides (Thermo Fisher) in neurobasal medium without phenol red (Gibco) at a density of 150,000 to 200,000 cells chamber^{-1}. Time-lapse images were acquired at 37 °C under a humidified 5% CO_2 atmosphere. A neurite length of 100 μm was selected in 10 neurons. To prevent phototoxicity, a 5 μm z-stack was acquired with 1 μm step size (2×2 binning) for each time point. The mitochondrial movement objective was recorded for 5 min with 5 s intervals. Each frame of the time-lapse stacks was de-hazed and maximum projected by a custom written journal in MetaMorph 7.5. The kymograph was generated with all planes, 25 μm line width, and average projected without background subtraction in Metamorph 7.5. The parameters of mitochondrial velocity and moving distance were imported into Excel for further analysis. Mitochondrial movements were classified as motile with velocity > 20 μm min^{-1} or stationary with velocity < 20 μm min^{-1}.

Confocal microscopy. Confocal microcopy was performed using a NikonA1R VAAS. Laser Point- and Resonant-Scanning Confocal Microscope equipped with a 32-channel spectral detection, deconvolution, ultra-sensitive VAAS detector, Perfect Focus (PFS), and a CFI Plan Apochromat VC 60× WI NA 1.20, W.D. 0.27 mm objective. Single

photon Ar-ion laser was emitted at 488 and 514 nm; Diode laser, emitting at 561 nm. Image acquisition and processing was performed using the Nikon Elements software.

Scoring of mitochondrial fragmentation and neuronal cell death. Primary cortical neurons were fixed two days after transfection and scored as described[1,3]. Scoring was done by two blinded individuals. Statistics: ANOVA post-hoc test. Fibroblasts were analyzed at day 6 after seeding at a density of 10,000 cell ml^{-1}. Mitochondria in human fibroblasts were visualized with MitoTracker Red CMXRos (100 nM).

Isolation of brain mitochondria from YAC18 and YAC128 mice. Brain mitochondria were isolated from 1.5 or 2 month mice by differential and gradient centrifugations as described[4]. Mitochondrial pellets were lysed in 0.7 ml of T-PER buffer (Thermo Scientific) with protease inhibitors (Roche). Protein concentrations were determined with the Quick Start Bradford assay (Bio-Rad). Mitochondrial lysates (150–200 µg) were used immediately for co-immune precipitation.

Isolation of mitochondria from human lymphoblasts. Mitochondria from human lymphoblasts were isolated as described[5] except that the mitochondrial pellet was lysed with 190 µl T-PER (Thermo Scientific) and protease inhibitors (Roche). Protein concentrations were determined with the Quick Start Bradford assay (Bio-Rad). Mitochondrial lysates (145 µg) were used for co-immune precipitation.

Preparation of postmortem human brain extracts. Samples were lysed as described with the following modifications[6]. The tissue was homogenized using a glass-Teflon homogenizer at maximum speed and five strokes. Homogenates were then sonicated (VirSonic 100, VirTis) three times for 5 s with 5 s intervals and centrifuged for 30 min at 15,000 rpm. The supernatants were pre-cleared with 75 µl Protein G Sepharose slurry (GE Healthcare). Samples were rotated for 2 h. Protein determination of the cleared extracts was performed with the BCA assay (Thermo Scientific). Extracts (2.5 mg) were used for immune precipitations.

Co-immune precipitation. All steps were carried out at 4 °C. Lysates were incubated overnight with 5 µl monoclonal mouse antibodies to HTT (MAB2166, clone 1HU-4C8, Millipore) and then incubated with 50 µl protein G sepharose (GE Healthcare) for 2 h. Unbound proteins were removed by washing 5 times with ice-cold PBS. Bound proteins were separated on NuPAGE 3%–8% Tris-Acetate gels (Invitrogen) under reduced conditions and transferred to nitrocellulose membranes (Hybond-ECL Nitrocellulose, 0.22 µm, GE Healthcare). Membranes were blotted with monoclonal mouse antibodies to DRP1 (clone 8/DLP1, BD Bioscience) (1:1,000) followed by sheep-anti-mouse IgG-HRP (GE Healthcare) (1:1,000) or goat-anti-mouse-HRP (Thermo Scientific) (1:3,000). Blots were probed for MFN2 with rabbit antibodies to MFN2 (M6444, Sigma) (1:1,000) and donkey-anti-rabbit IgG-HRP (GE Healthcare) (1:5,000) as the secondary antibody or mouse antibodies to MFN2 (XX-1, Santa Cruz) (1:250) and sheep-anti-mouse IgG-HRP (GE Healthcare) (1:2,000) antibodies. Control immune precipitations were carried either without antibodies or 5 µl donkey-anti-mouse IgG (Jackson Immuno Research Lab) or 5

µl unaffected mouse IgG (Upstate) as negative controls. DRP1 immune precipitations were carried out with 6 µl monoclonal mouse DRP1-specific antibodies (Clone 8/DLP1, BD Bioscience) or 15 µl polyclonal rabbit DRP1-specific antibodies (H-300, Santa Cruz), and membranes were blotted with monoclonal mouse HTT-specific antibodies (MAB2166, clone 1HU-4c8, Millipore) (1:1,000). The intensities of the signals were determined using Image J 1.6.0_10, normalized to the input signals, and expressed as arbitrary units. The arbitrary units shown below the Western blot have been normalized with the input.

Cloning, expression, and purification of bacterial DRP1 protein. Cloning of human DRP1 (NCBI accession number: NM_012062.3) into the *E. coli* expression vector pET21 (Novagen) was performed using Nde I and Xho I restriction sites resulting in the attachment of a C-terminal 6× His-tag. Plasmids were transformed using *E. coli* BL21 (DE3) star cells (Stratagene) and expression was performed at 25 °C overnight by induction with 0.5 mM IPTG. Cells were harvested by centrifugation and resuspended in 50 mM KH_2PO_4, 300 mM NaCl, 5 mM imidazole, 0.1 mg ml^{-1} lysozyme, 10% glycerol (pH 7.8). Lysis was performed by sonication using a Sonoplus HD2070 (Bandelin). Soluble 6×-His tagged proteins were loaded on Ni-NTA resin, washed with 20 mM Tris, 300 mM NaCl, 40 mM imidazole, 10% sucrose, 10% glycerol (pH 7.8) and eluted with 25 mM Tris, 300 mM NaCl, 500 mM imidazole, 10% glycerol (pH 7.8). DRP1 containing fractions were further injected onto a Superdex 200 10/300 GL Äkta FPLC column (GE Healthcare) equilibrated with 30 mM Tris, 100 mM NaCl, 2 mM DTT, 1 mM EDTA (pH 7.8). Purified proteins were stored at –80 °C.

Isolation of baculovirus DRP1 protein. DRP1 (NCBI accession number: NM_005690.3, with 699 amino acid residues plus N-6 His tag) was produced using baculovirus SF9 cell expression system. Four liters of SF9 cells were infected with DRP1-containing virus at MOI of 5 and incubated for 48 hours. Cells were collected by centrifugation and resuspended in the lysis buffer (50 mM Tris pH 8.0, 150 mM NaCl, 1 mM PMSF) containing protease inhibitors (Sigma). Cell lysis was performed using an Emulsiflex-C3 homogenizer (Avestin). The soluble proteins were then recovered and loaded on a 5 ml Ni-NTA (Novagen) affinity column. The column was washed with 20 mM Tris (pH 8.0), 1.0 M NaCl, and 5 mM imidazole buffer, and then with 20 mM Tris (pH 8.0), 150 mM NaCl, and 5 mM imidazole. DRP1 was eluted with 20 mM Tris (pH 8.0), 150 mM NaCl, and 300 mM imidazole. Fractions containing DRP1 were combined and loaded on a Superdex 200 16/60 FPLC column (GE Healthcare) equilibrated with 20 mM Hepes (pH 7.5) and 150 mM NaCl. Purified DRP1 was eluted in 20 mM HEPES (pH 7.5), 150 mM NaCl, 10% glycerol and stored at –80°C.

Preparation of bacterial HTT exon1 proteins. BL21 bacteria transformed with GST-HTT exon1-Q20, GST-HTT exon1-Q53 were grown overnight in Luria-Bertani (LB) medium with ampicillin at 37 ^{o}C. Expression was induced with 1 mM IPTG for 4 h at 30 ^{o}C. Soluble fusion proteins were purified as described[7], concentrated with an Amicon ultra centrifugal filter, Ultracel 30K (Millipore), and stored at –80^{o}C.

EM negative stain. Purified baculovirus DRP1 (NCBI accession number: NM_005690.3) was dialyzed overnight in the absence of glycerol and presence of 1 mM DTT. Incubation was performed on ice at a DRP1 concentration of 0.4 mg ml^{-1} with or without 0.2 mg ml^{-1} Q20-GST or Q53-GST with 2 mM $MgCl_2$ in the absence or presence of 2 mM nucleotide GTP, GDP, and GMP-PNP. Nucleotides were purchased from Sigma. Samples were further diluted by a factor of 50× in appropriate buffer and applied to glow-discharged carbon coated EM grids stained with 2% uranyl acetate and observed using a Tecnai 12 microscope (FEI electron optics) equipped with a Lab6 filament at 120 kV. Images were acquired on a Gatan 792 Bioscan 1k × 1k Wide Angle Multiscan CCD Camera.

EM and stereology. Mice were anesthetized with Avertin and intracardiac perfusion was performed on 2- or 6-month-old FVB/N or YAC128 mice (n = 3). The experiment was performed twice. Fixation was done with 2% paraformaldehyde, 2.5% glutaraldehyde, and 0.15 M sodium cacodylate, pH 7.4 at 37 °C for 3–5 min. Brains were removed and placed in the fixative solution for 1 h on ice. Brains were sliced in 100 µm thick sections, placed in ice-cold fixative solution, rinsed with 0.15 M sodium cacodylate (Ted Pella) and 3 µM calcium chloride, and post-fixed for 1 h in ice-cold 1% osmium tetroxide (Ted Pella), 0.8% potassium ferrocyanide, and 3 µM calcium chloride in 0.15 M sodium cacodylate. Sections were stained overnight with 2% uranyl acetate at 4 °C. After serial dehydration, sections were infiltrated in 50% ethanol-50% Durcupan resin (Fluka) followed by 100% Durcupan. Finally, after polymerization at 60 °C for 72 h under vacuum, the striata were dissected, sliced in ultra-thin sections (70 nm), and post-stained

with 2% uranyl acetate and lead salts before examination with a JEOL 1,200FX electron microscope operated at 80 kV. Images were recorded on film at magnifications of 5,000× or 6,000×. Negatives were digitized at 1,200 dpi with a Nikon CoolScan. Micrographs were analyzed using Image J software and mitochondrial length was measured as described[8].

EM tomography. For tomographic reconstructions, a series of tilt images were acquired using a JEOL 4000 EX intermediate high-voltage electron microscope operated at 400 kV as described[9,10].

MOM liposome preparation. L-α-phosphatidylcholine (PC), Cardiolipin (CL), L-α-phosphatidylethanolamine (PE), L-α-phosphatidylinositol (PI) were purchased in chloroform solution from Avanti Polar Lipids, Inc. and mixed at a ratio of 52: 6: 22: 20 by weight to mimic MOM composition[11]. The chloroform was removed by a stream of nitrogen and the lipid film was evaporated using a vacuum chamber for at least 1 hr at room temperature. The lipid film was then re-hydrated in 25 mM HEPES and 25 mM PIPES, pH 7.0 at room temperature for 1 h to yield 5 mg ml^{-1} lipids and five cycles of freezing in liquid nitrogen and thawing at 30 ^{o}C using a water bath were performed. Last, the lipids were extruded using an Avanti Polar Lipid extruder with 15 repetitions and a 0.8 μm polycarbonate membrane (Whatman) and stored in the dark at 4 ^{o}C until use.

DRP1 GTPase assay. DRP1 GTPase activity was measured with the continuous method and the data was analyzed as described[12]. A ratio of 0.5 μM of recombinant bacterial

DRP1 (NCBI accession number: NM_012062.3) to 0.2 mg ml^{-1} MOM liposomes were pre-incubated at room temperature for 20 min in HEPES/PIPES buffer, then 0.4 µM of GST-HTT exon1 protein isolated from bacteria was added and incubated at room temperature for another 20 min. GTPase activity was determined for nine GTP concentrations (0, 0.01, 0.02, 0.03, 0.05, 0.1, 0.25, 0.5, and 1.0 mM) and the absorbance at 340 nm was measured at 30 ^{o}C for 100 cycles of 60 s each with a FLUOstar Galaxy (BMG Labtechnologies) plate reader. The path length under the assay conditions in the Falcon MICROTEST plate was 0.38 cm.

Direct interaction of DRP1 and HTT in vitro. Recombinant DRP1 protein (0.5 µM) was pre-incubated with MOM liposomes (0.2 mg mL^{-1}) in 25 mM HEPES/PIPES buffer (pH 7.0) for 20 min at room temperature and followed by the addition of GST-HTT exon1-20Q or -53Q fragments (0.1, 0.2, 0.3 µM) and another 20 min incubation. Mixtures were immune precipitated with monoclonal mouse DRP1-specific antibodies (clone 8/DLP1, BD Bioscience) (1:400) and Western blots were probed with monoclonal mouse HTT specific antibodies (MAB5492, clone 2B4, Millipore) (1:1,000).

References for Supplementary Information

1. Barsoum, M.J., *et al.* Nitric oxide-induced mitochondrial fission is regulated by dynamin-related GTPases in neurons. *Embo J* **25**, 3900-3911 (2006).
2. Liot, G., *et al.* Complex II inhibition by 3-NP causes mitochondrial fragmentation and neuronal cell death via an NMDA- and ROS-dependent pathway. *Cell Death Differ* **16**, 899-909 (2009).
3. Song, W., *et al.* Assessing mitochondrial morphology and dynamics using fluorescence wide-field microscopy and 3D image processing. *Methods* **46**, 295-303 (2008).
4. Brustovetsky, N., Brustovetsky, T., Jemmerson, R. & Dubinsky, J.M. Calcium-induced cytochrome c release from CNS mitochondria is associated with the permeability transition and rupture of the outer membrane. *J Neurochem* **80**, 207-218 (2002).
5. Bossy-Wetzel, E. & Green, D.R. Assays for cytochrome c release from mitochondria during apoptosis. *Methods Enzymol* **322**, 235-242 (2000).
6. Kaltenbach, L.S., *et al.* Huntingtin interacting proteins are genetic modifiers of neurodegeneration. *PLoS Genet* **3**, e82 (2007).
7. Wanker, E.E., *et al.* Membrane filter assay for detection of amyloid-like polyglutamine-containing protein aggregates. *Methods Enzymol* **309**, 375-386 (1999).

8. Perkins, G.A., *et al.* Electron tomographic analysis of cytoskeletal cross-bridges in the paranodal region of the node of Ranvier in peripheral nerves. *J Struct Biol* **161**, 469-480 (2008).

9. Perkins, G.A., *et al.* Electron tomography of mitochondria after the arrest of protein import associated with Tom19 depletion. *Eur J Cell Biol* **80**, 139-150 (2001).

10. Perkins, G.A., *et al.* Electron tomography of mitochondria from brown adipocytes reveals crista junctions. *J Bioenerg Biomembr* **30**, 431-442 (1998).

11. Daum, G. Lipids of mitochondria. *Biochim Biophys Acta* **822**, 1-42 (1985).

12. Ingerman, E. & Nunnari, J. A continuous, regenerative coupled GTPase assay for dynamin-related proteins. *Methods Enzymol* **404**, 611-619 (2005).

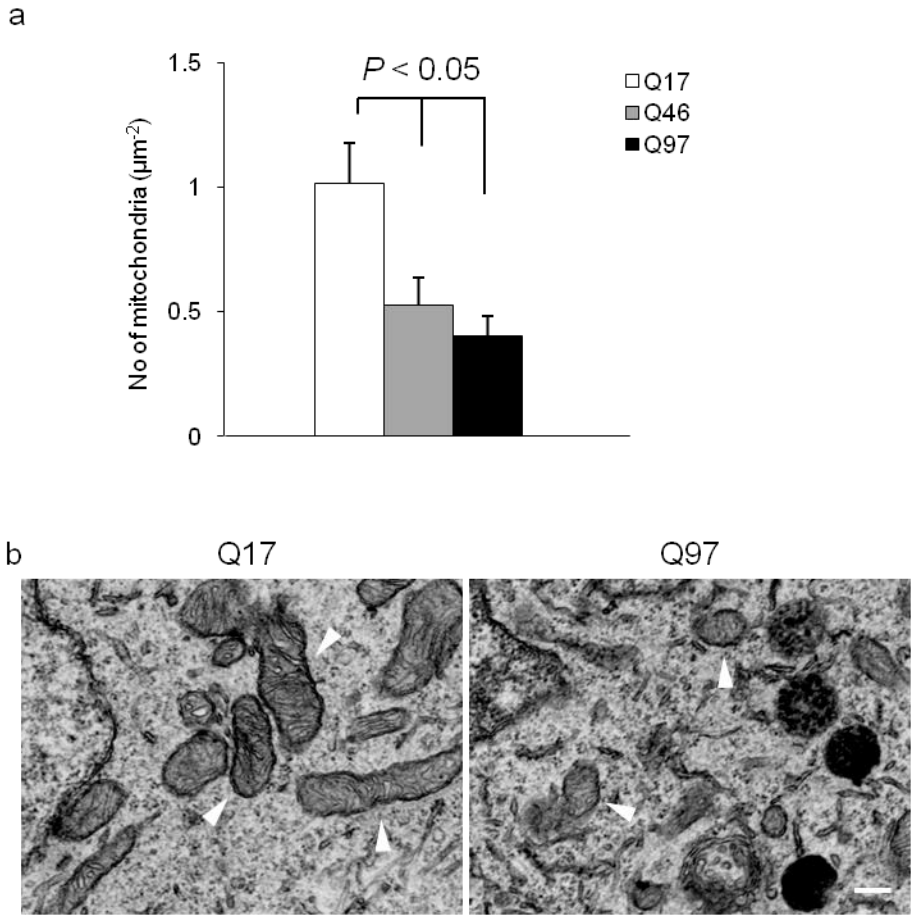

Supplementary Figure 1 The number of mitochondria decreases in neurons expressing mutant *HTT*. (**a**) Number of mitochondria per square µm of cytoplasmic area in cortical neurons expressing *HTT* exon1-Q17, -Q46, or -Q97. Data are mean ± s.e.m. Statistics: ANOVA one-way test. (**b**) Representative EM micrographs of primary cortical neurons expressing *HTT* exon1-Q17 or -Q97. Mitochondria are indicated with white arrowheads. Scale bar, 200 nm.

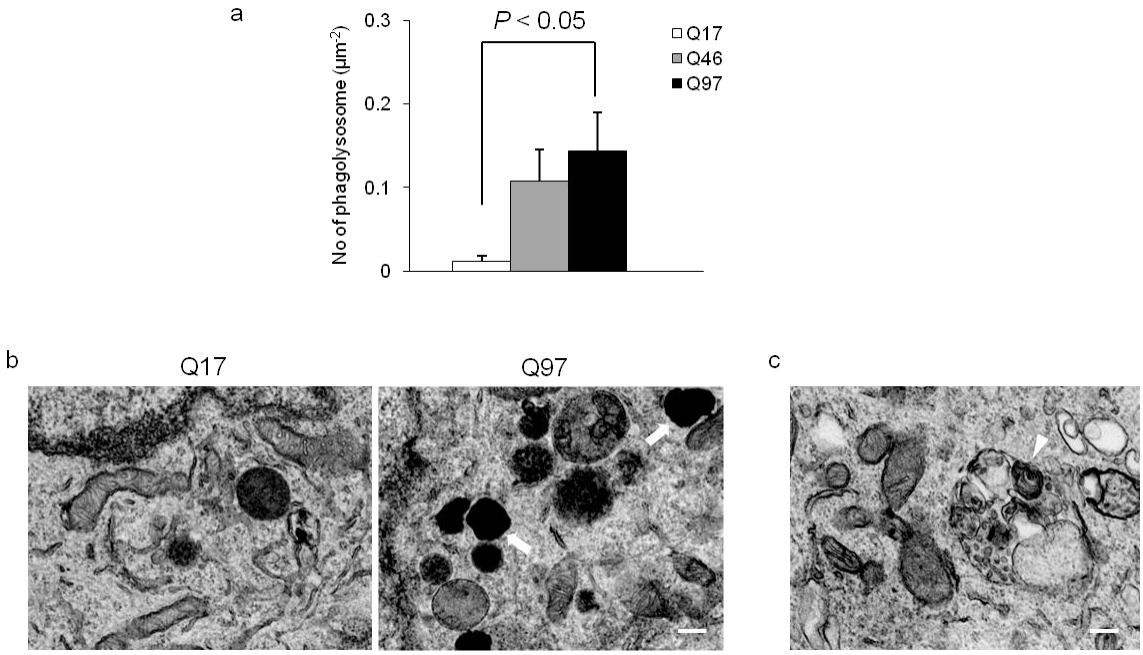

Supplementary Figure 2 Mutant HTT increases the number of phagolysosomes. (**a**) Number of phagolysosomes (μm^{-2}) of cytoplasmic area in primary cortical neurons expressing *HTT* exon1-Q17, -Q46, or -Q97. Data are mean ± s.e.m. ANOVA one-way test. (**b**) EM of primary cortical neurons expressing *HTT* exon1-Q17 or -Q97 showing phagolysosomes (white arrows). (**c**) EM micrograph of an autophagosome containing a mitochondrion (white arrowhead). Autophagosomes containing mitochondria were rare, owing to the short-lived nature of these structures. Scale bar, 200 nm.

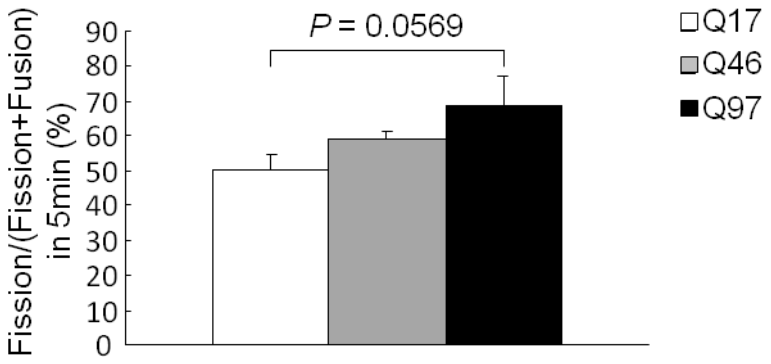

Supplementary Figure 3 Increased ratio of fission to fission plus fusion events in mutant *HTT* (Q46 and Q97) expressing neurons. Neurons were transfected with vectors coding DsRed2-Mito and *HTT* exon1-Q17, -Q46, or -Q97 and mitochondria fission and fusion events were recorded for 5 min (n = 10, = 10, = 5, for *HTT* exon1-Q17, -Q46, and -Q97, respectively). Data are mean ± s.e.m. Statistics: ANOVA one-way test.

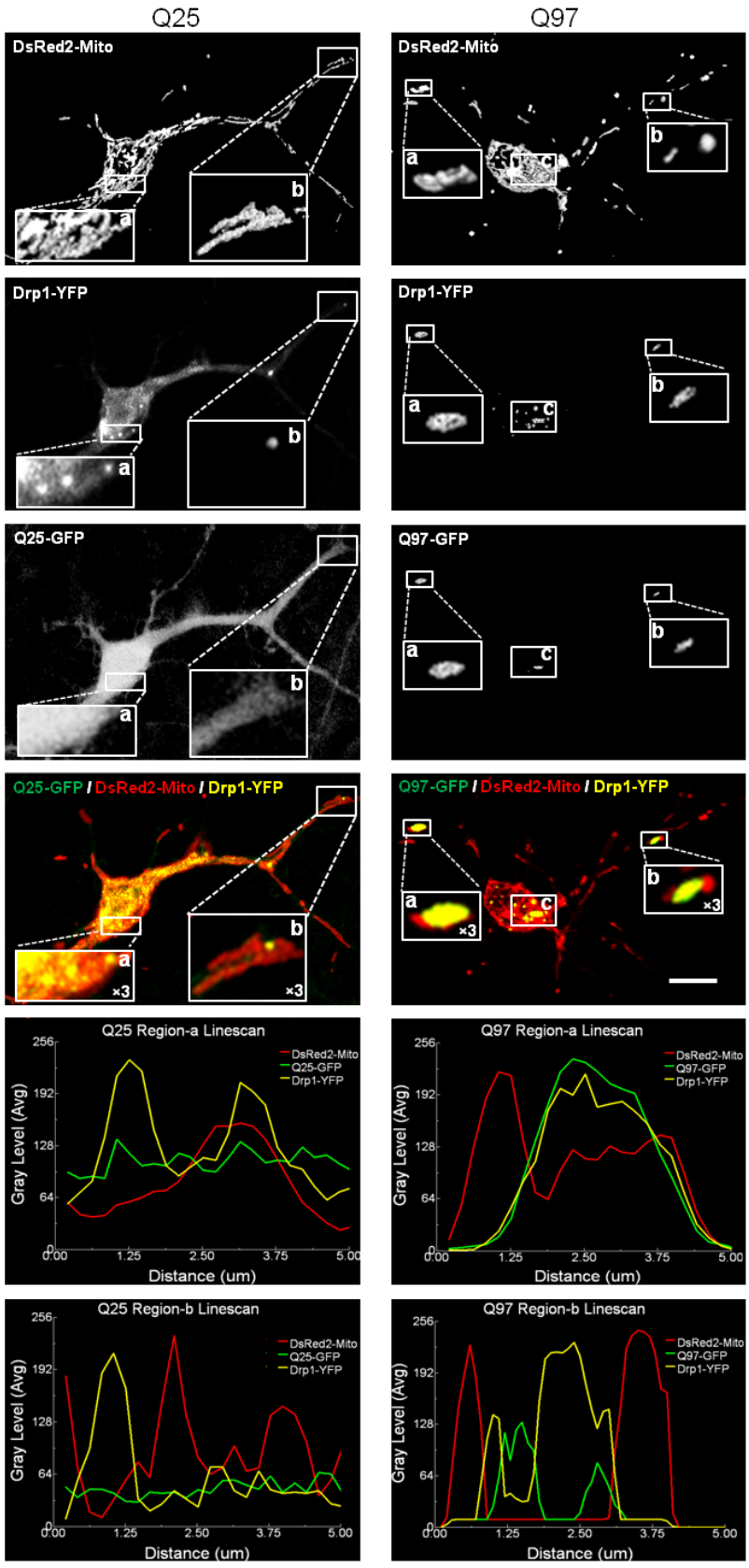
Q25
Q97
DsRed2-Mito
Drp1-YFP
Q25-GFP
Q97-GFP
Q25-GFP / DsRed2-Mito / Drp1-YFP
Q97-GFP / DsRed2-Mito / Drp1-YFP
Q25 Region-a Linescan
Q97 Region-a Linescan
Q25 Region-b Linescan
Q97 Region-b Linescan
Gray Level (Avg)
Distance (um)
256
192
128
64
0.00
1.25
2.50
3.75
5.00

Supplementary Figure 4 Mutant HTT exon1-Q97 co-localizes with DRP1 on mitochondria. Cortical neurons were co-transfected with expression vectors encoding DsRed2-Mito, *DRP1*-YFP and *HTT* exon1-GFP. After two days of transfection neurons were fixed and analyzed by confocal microscopy. Shown are the confocal images corresponding to **Fig. 3b** with the DsRed2, YFP, and GFP channels presented separately and additional line scans. While normal HTT (Q25) reveals poor colocalization with DRP1, clear co-localization is observed with mutant HTT (Q97) either on mitochondria or as bridge between two fragmented mitochondria shown by the images of each channel and the line scans, which reveal overlapping peaks in DRP1-YFP and HTT exon1-GFP fluorescent signals. ×3 zoom of boxed regions. Scale bar, 10 μm.

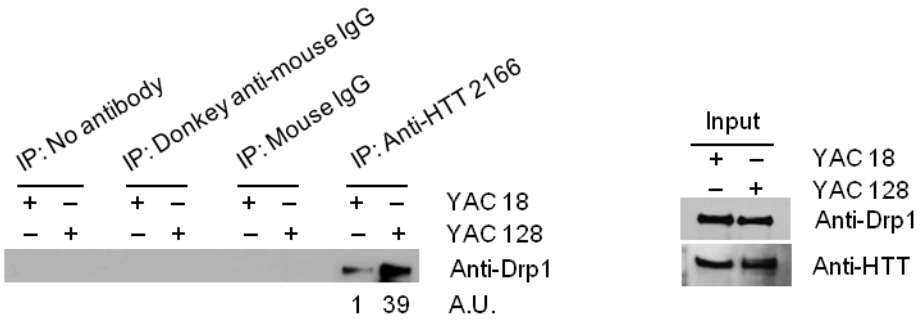

Supplementary Figure 5 Specificity of the mutant HTT-DRP1 co-immune precipitations. Immune precipitation of brain mitochondrial lysates isolated from four month-old YAC18 or YAC128 mice with protein G Sepharose lacking antibodies or negative control antibodies including donkey-anti-mouse IgG (Jackson Immuno Research Lab), normal mouse IgG (Upstate), or mouse HTT-specific antibodies (MAB2166, clone 1HU-4C8, Millipore) and Western blots were probed with Drp1-specific antibodies (clone 8/DLP1, BD Bioscience). Intensities of signals are shown as arbitrary units (A.U.) and were normalized to input signals.

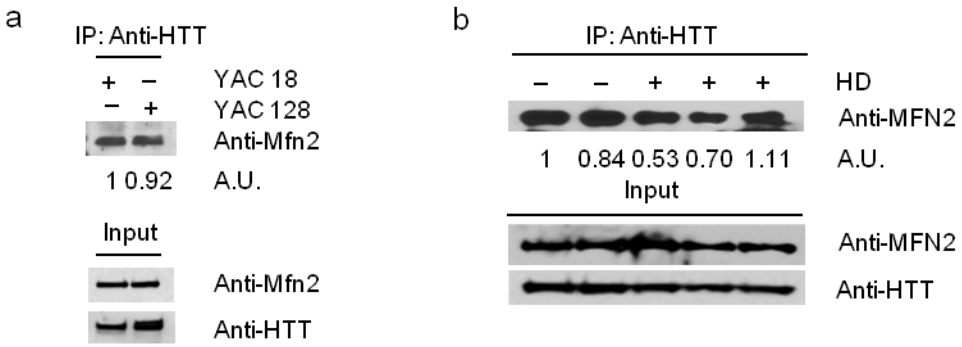

Supplementary Figure 6 Mutant HTT does not form an increased complex with MFN2 in HD mice or HD individuals. (**a**) Immune precipitations of mitochondrial brain lysates isolated from five weeks old YAC18 and YAC128 mice with HTT-specific antibodies followed by Western blotting using Mfn2-specific antibodies. Intensities of signals are shown as arbitrary units (A.U.) and were normalized to input signals. (**b**) Immune precipitations of mitochondrial lysates from normal and HD human lymphoblasts with HTT-specific antibodies followed by Western blotting with MFN2-specific antibodies.

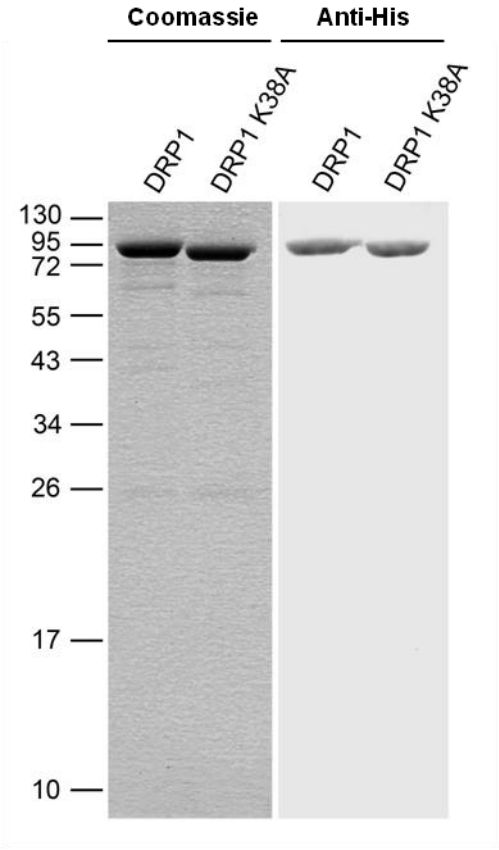

Supplementary Figure 7 SDS-PAGE and Western blot analysis of human DRP1 protein (NCBI accession number: NM_012062.3) expressed *in E. coli*. Purified proteins were separated by 15% SDS-PAGE and gels were either stained with Coomassie Blue, or for Western blotting, mouse penta His-specific antibodies (Qiagen) were used.

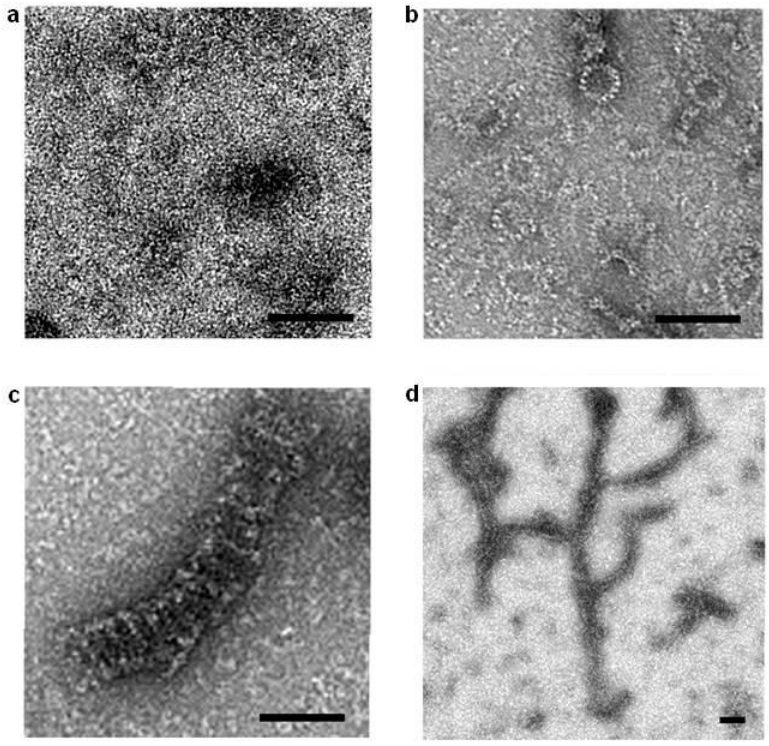

Supplementary Figure 8 DRP1 self-assembles in solution into ring- and spiral-like oligomers. Negative EM micrographs of baculovirus DRP1. (**a**) DRP1 in the absence of nucleotides. (**b**) Ring-like DRP1 oligomers of 35 ± 5 nm in diameter in the presence of 2 mM GTP. (**c**) Spiral-like DRP1 oligomers in the presence of 2 mM GMP-PNP, non-hydrolyzing analog of GTP. (**d**) Spiral-like DRP1 oligomers with length of several hundred nanometers. Scale bars, 50 nm.

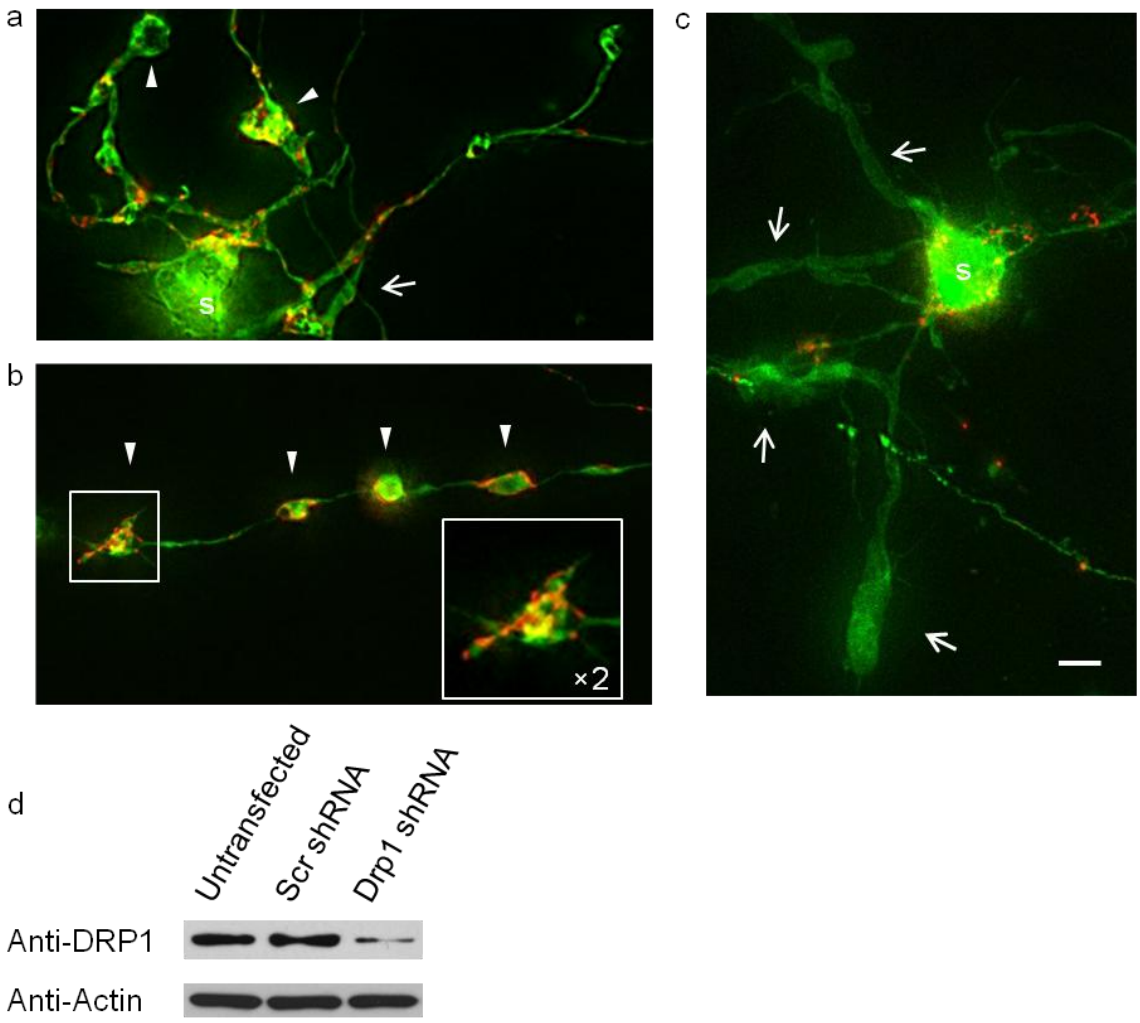

Supplementary Figure 9 DRP1 knockdown by *DRP1* shRNA expression alters neuronal development of cortical neurons (7 DIV). (**a**) Abnormal neurite morphology indicated by the white arrow and arrowhead of a primary cortical neuron expressing DsRed2-Mito, *HTT* exon1-Q17, and DRP1 shRNA. (**b**) Abnormal flat disks in neurites indicated by the white arrowhead in a neuron expressing DsRed2-Mito, *HTT* exon1-Q17, and *DRP1* shRNA. (**c**) Abnormal widening of neurites that are devoid of mitochondria (white arrow) in a neuron expressing DsRed2-Mito, *HTT* exon1-Q17, and *DRP1* shRNA. Scale bar, 10μm. (**d**) Western blot of DRP1 demonstrating effective DRP1 knockdown in rat C6 glioma cells two days after transfection.

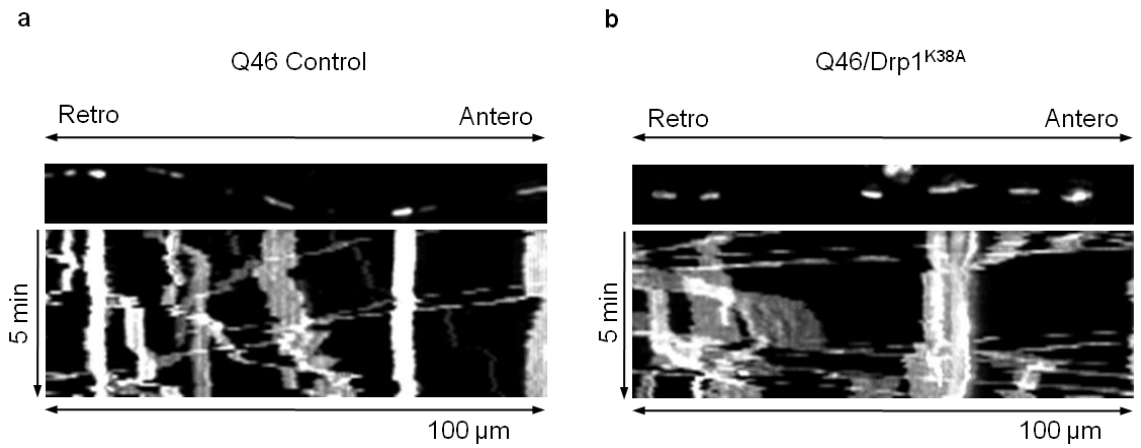

Supplementary Figure 10 DRP1^{K38A} rescue of mitochondrial transport defects in neurites of cortical neurons. (**a**) Representative kymograph of neurons transfected with *HTT* exon1-Q46 and DsRed2-Mito. (**b**) Representative kymograph of neurons transfected with *HTT* exon1-Q46, DsRed2-Mito, and additional *DRP1*^{K38A}.

Supplementary Table 1 Table of DRP1 and DRP1^{K38A} GTPase enzymatic parameters including GTPase activities at 0.05 mM GTP, maximal rate of GTP hydrolysis (V_{max}), and apparent Michaelis-Menten constant (K_m).

	Activity at 0.05 mM GTP (min^{-1})	**Vmax ($\times 10^{-6}$ M min^{-1})**	**Km (mM)**
DRP1+ Q20	**2.03 ± 0.317***	**2.72 ± 0.196***	**0.092 ± 0.0129****
DRP1+ Q53	**2.49 ± 0.532***	**2.96 ± 0.311***	**0.077 ± 0.0134****
DRP1^{K38A} + Q20	**0.268 ± 0.032**	**N/A**	**N/A**
DRP1^{K38A} + Q53	**0.294 ± 0.048**	**N/A**	**N/A**

Data represent the mean values and S.D. from three independent measurements. Student's *t*-test was used for statistical analysis, $P < 0.05$*, $P < 0.01$**.

Supplementary Movie Legends

Supplementary Movie 1. Mitochondrial movement in a neuron expressing *HTT* exon1-Q17-GFP and DsRed2-Mito. Movie corresponds to the kymograph in **Fig 1f**, top panel and shows mitochondrial transport. The movie lasts 5 min and is played back accelerated (original: 5 s frame^{-1}, playback: 1/6 s frame^{-1}).

Supplementary Movie 2. Mitochondrial movement in a neuron expressing *HTT* exon1-Q46-GFP and DsRed2-Mito. Movie corresponds to the kymograph in **Fig 1f**, center panel and shows a clear decrease in mitochondrial transport. The movie lasts 5 min and is played back accelerated (original: 5 s frame^{-1}, playback: 1/6 s frame^{-1}).

Supplementary Movie 3. Mitochondrial movement in a neuron expressing *HTT* exon1-Q97-GFP and DsRed2-Mito. Movie corresponds to the kymograph in **Fig 1f**, bottom panel and shows more pronounced arrest in mitochondrial transport. The movie lasts 5 min and is played back accelerated (original: 5 s frame^{-1}, playback: 1/6 s frame^{-1}).

Supplementary Movie 4. Electron tomography of a control mitochondrion in a medium spiny neuron. Movie showing the three-dimensional details of a mitochondrion in a medium spiny neuron reconstructed using electron tomography. These mitochondria are typically elongated along the direction of the axonal long axis. **Clip 1**: A rapid sequence through 190 slices (2.2 nm slice^{-1}) of the tomographic volume that shows nearly the entire mitochondrial volume. There are 84 cristae. **Clip2**: Rotations and zooms of the

surface-rendered volume after segmentation of the inner and outer membranes. The blue outer membrane is translucent to visualize the cristae displayed in various colors. **Clip3:** Rotation of the cristae after removal of the outer membrane to better distinguish the variety of shapes and sizes.

Supplementary Movie 5. Electron tomography of a fissioning YAC128 mitochondrion in a medium spiny neuron. Movie showing the three-dimensional details of a mitochondrion fissioning into three parts in a medium spiny neuron reconstructed using electron tomography. **Clip 1**: A rapid sequence through 210 slices (2.2 nm slice^{-1}) of the tomographic volume. There are 223 cristae, many of which are small. **Clip2**: Rotation showing the outer membrane and the widths of the two constriction sites. **Clip3:** Rotations showing the cristae in each of the three parts. **Clip4:** Rotations and zooms highlighting the cristae and the constriction sites. The blue outer membrane is translucent to visualize the cristae displayed in various colors.